# Measurements of $F_2$ and $xg$ at HERA

Max Klein

representing the H1 and ZEUS Collaborations

DESY-IfH Zeuthen, Platanenallee 6, D-15738 Zeuthen

**Abstract:**

Based on data taken at the $ep$ collider HERA in 1993, measurements are discussed of the proton structure function $F_2(x, Q^2)$ and of the gluon distribution $xg(x, Q^2)$ as derived from QCD analyses of the scaling violation of $F_2$. The measurements of the H1 and ZEUS experiments explore a new kinematic range down to Bjorken $x$ of $2 \cdot 10^{-4}$ and up to four-momentum squared, $Q^2$, of 4000 $GeV^2$. They are in agreement with each other and with data from the fixed target deep inelastic scattering experiments at higher $x$ and lower $Q^2$ values. The observed rise of $F_2$ and of $xg$ towards lower $x$ values and the logarithmic $Q^2$ dependence of the structure function are in accord with perturbative QCD.

## 1 Introduction

Deep inelastic scattering (DIS) experiments of leptons off protons have made major contributions to the investigation of the strong interactions at small distances. Early electroproduction experiments have discovered the pointlike proton substructure by observing a scale invariant dependence of the proton structure function $F_2(x, Q^2)$ on the four-momentum transfer squared $Q^2$ at large $x \geq 0.1$ and $Q^2$ values of about 5 $GeV^2$. Subsequent neutrino scattering experiments have established the Quark Parton Model (QPM) considering valence and sea quarks as the constituents of the proton. The interaction of these partons as mediated by gluons is successfully described by Quantum Chromodynamics which has been tested with high precision in muon-nucleon DIS experiments.

HERA is the first electron-proton collider ever built. It extends the previous investigations in fixed target experiments into a new kinematic region. With electrons of energy $E_e = 26.7\ GeV$ and protons of $E_p = 820\ GeV$ the kinematic range presently explored extends to high $Q^2 \simeq 4000\ GeV^2$ and to very small $x$ values $\simeq 10^{-4}$ as $x = Q^2/sy$ with the inelasticity variable $y$ and the cms energy $s = 4E_eE_p$. The two large collider experiments H1 [1] and ZEUS [2] completely reconstruct the scattered electron kinematics and the hadronic final state, apart from losses near the beam pipe ($\theta_e \geq 173^o$ for nominal vertex position and $\theta_h \geq 10^o$ for the data of the year 1993 reported here). Since the inclusive DIS cross section depends on two variables only, the measurement of the scattered electron energy $E_e'$ and angle $\theta_e$, of the hadronic quantity $\sum_h = \sum_i (E_i - p_i^z)$ and of the hadron angle $\theta_h$ allows the redundant determination of the kinematics and as well maximum coverage of the available $(x, Q^2)$ range. Here $tan\theta_h/2$ is defined as $\sum_h / p_T^h$ with $p_T^h = \sqrt{(\sum_i p_x^i)^2 + (\sum_i p_x^i)^2}$ and the summations extend over all particles but the scattered electron. This report summarizes the measurements and QCD analyses of the proton structure function $F_2(x, Q^2)$ by the H1 [3] and ZEUS [4] collaborations based on data collected in the year 1993 where HERA delivered an integrated luminosity of about 1 $pb^{-1}$.

## 2 Measurement of the Proton Structure Function $F_2(x, Q^2)$

Various methods can be employed to reconstruct the event kinematics. In the 'electron method' $Q^2$ and $x$ are determined as functions of $E_e'$ and $\theta_e$. The method is not purely electron based as hadrons are used also to reconstruct the event vertex and, in part of the analyses, to impose an energy momentum constraint, i.e. $\sum_{all}(E - p_z) \simeq 2E_e \cdot (1 - y_e + y_h)$ reducing background and radiative events. The electron method ensures best resolution of $\delta Q^2 \leq 5\%$ in the full kinematic plane and of $\delta x \simeq 10\%$ for $y \geq 0.1$. However, it implies radiative corrections of up to about 30% at low $x$. At larger $x$ the resolution degrades as $1/y \cdot \delta E_e'/E_e'$. Thus $y_e$ has been replaced by $y_h = \sum_h / 2E_e$. Replacing $2E_e$ by $\sum_{all}(E - p_z)$ one defines $y_\Sigma$ and modifies $Q_e^2 = {p_T^e}^2/(1 - y_e)$ to $Q_\Sigma^2 = {p_T^e}^2/(1 - y_\Sigma)$. This '$\Sigma$ method' is rather insensitive to corrections due to initial state photon radiation. At low $y \leq 0.1$ the $\Sigma$ method is equivalent to the mixed method which combines $Q_e^2$ and $y_h$ to define $x$. The 'double angle method' relies on a measurement of the scattering angles $\theta_e$ and $\theta_h$ which reduces the influence of energy scale uncertainties. Approximately $\theta_h$ is the energy weighted mean of the polar angles of the final state particles [5]. The double angle method can be used over the full kinematic range albeit with limited resolution ($\geq 30\%$) at smallest $x \leq 5 \cdot 10^{-3}$. H1 has combined the electron and $\Sigma$ method to determine $F_2$ using the double angle method as a cross check. ZEUS opted for the double angle method for their final $F_2$ using the electron method as a cross check.

A $1-2\%$ precision for $E_e'$ was achieved adjusting the calibrated calorimeter response with the help of the angular measurements, i.e. $E_e' = E(\theta_e, \theta_h)$ for $\theta_h$ around $40^o$. Important cross checks on the $E_e'$ determination and the measurement resolution arise from the "kinematic peak shape", a cross section singularity at $x = E_e/E_p \simeq 0.03$ where $E_e' \simeq E_e$, and from the elastic Compton scattering events $ep \rightarrow e\gamma p$ with the relation $E_e' + E_\gamma = E_e$. The polar angle $\theta_e$ is measured with a few *mrad* precision using the reconstructed vertex position and the tracker (H1) or the calorimeter (ZEUS, also H1 for their high $Q^2 \geq 150\ GeV^2$ data). A huge background from strong proton beam wall and beam gas interactions is suppressed to below the 1% level by calorimeter timing to about 1 *ns* (ZEUS) or by vertex and time-of-flight requirements (H1). This is checked by analyses of the noncolliding "pilot" bunches. Physics background is due to very small $Q^2$ photoproduction processes in which the scattered electron escapes detection but electromagnetic energy, deposited in mostly the backward calorimeters, mimics a DIS electron. This background extends locally to $5-10\%$ complicating the $F_2$ measurements at very large $y$ (small $E_e' \leq 7\ GeV$). The amount of photoproduction background can presently be estimated to 50% accuracy by analyzing the about 20% of photoproduction events in which the scattered electron is recognized in the electromagnetic calorimeter about 35 *m* downstream the electron beam. Altogether the systematic errors are about 10-15% with no single dominating error source.

The event samples used in 1993 by ZEUS and H1 comprise 46 *k* or 24 *k* events for a luminosity of 0.54 or 0.27 $pb^{-1}$, respectively. The kinematic cuts are defined in [3, 4]. The luminosity error is kept separately from the quoted errors and amounts to 3.5% for ZEUS and 4.5% for H1, mainly due to uncertainties of the electron tagger acceptance. Enlarged statistics in 1994 and refined calibration mean that the systematic errors can be reduced by about a factor of two. Upgrades of the H1 and ZEUS detectors are being performed to measure $F_2$ at the per cent level of accuracy.

## 3 Results

The proton structure function $F_2(x, Q^2)$ is obtained from the measured deep inelastic scattering cross section after acceptance corrections based on detailed detector and physics simulations [3, 4] and after correction for higher order processes as photon bremsstrahlung and also $Z$ boson exchange effects. The cross section also depends on the structure function $2xF_1$. The ratio $R = F_L/2xF_1$ has been calculated according to QCD which relates the longitudinal structure function $F_L = F_2 - 2xF_1$ to the gluon distribution $xg$. Thus a large gluon distribution at low $x$ ($xg \sim 30$, see below) implies the ratio $R$ to be large ($R \sim 0.3$).

The measurements of $F_2$ by H1 and ZEUS are in good agreement with each other and with extrapolations from data of the fixed target experiments BCDMS [7], NMC [6] (figs. 1,2) and E665 [8] not shown here. The low $y \simeq 0.01$ data from H1 approach the NMC data for $Q^2 \sim 15\ GeV^2$. Genuine overlap with fixed target data, however, requires HERA to run at reduced beam energies which must be done to measure $R$. Both experiments established the previously observed rise of $F_2$ towards low $x$. This rise is more pronounced at large $Q^2$ but still sizeable at smallest $Q^2$, which were reached by H1 with a small data sample with the vertex position shifted by 70 *cm* downstream the $p$ beam. Around $Q^2 \simeq 5\ GeV^2$ $F_2$ is about twice larger than a flat extrapolation of NMC data would expect it to be (fig.1). An increase of $F_2$ at low $x$ has been predicted in asymptotically free field theories 20 years ago [9]. The low $x$ dependence of $F_2$ is related to the total virtual photoproduction cross section as $Q^2 \cdot \sigma_{tot}(\gamma^* p) \propto F_2(W, Q^2)$ where W is the invariant mass of the virtual photon proton system. Since $W^2 \simeq Q^2/x$ a rise of $F_2$ at low $x$ directly transforms into a rise

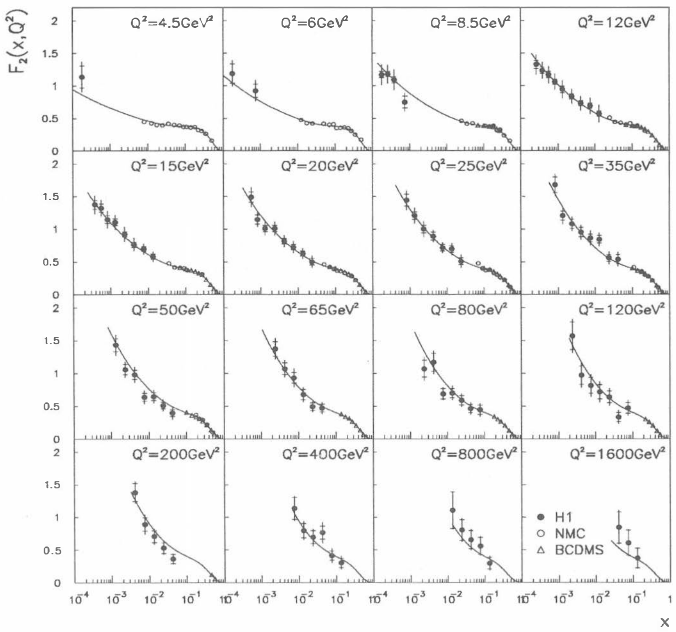


Figure 1: $F_2(x, Q^2)$ *measurement and NLO DGLAP QCD fit of H1.*

of $\sigma_{tot}(\gamma^* p)$ at large $W$ which is in contrast to the behaviour of the real photon-proton scattering cross section. The data of ZEUS and H1 contain a fraction of about 10-15% of diffractive events which are a genuine part of the inclusive DIS cross section measurement.

## 4 QCD and Determination of the Gluon Distribution xg

It has to be questioned whether the standard QCD $Q^2$ evolution equations [10] hold down to very low $x$ where $ln(1/x)$ terms become important [11] and large parton densities might necessitate the introduction of nonlinear terms in the evolution [12]. Both H1 [13] and ZEUS [14] have performed QCD fits to study that question and measure the gluon distribution at low $x$. The DGLAP equations represent a coupled system of integro-differential equations for the gluon distribution and the nonsinglet (NS) and singlet part (SI) of $F_2$ which in the DIS renormalization scheme and the QPM can be decomposed as $F_2 = (Q_u^2 + Q_d^2)/2 \cdot \sum(q + \overline{q}) + (Q_u^2 - Q_d^2)/2 \cdot \sum(q - \overline{q}) = 5/18\ (SI) + 1/6\ (NS)$ for 4 flavours. Here $Q_{u,d}$ denote the up and down quark charges and $q, \overline{q}$

| | ZEUS | H1 |
|---|---|---|
| data | $F_2^p(ZEUS, NMC), F_2^d(NMC)$ | $F_2^p(H1, NMC, BCDMS)$ |
| $Q_o^2$ | $7\ GeV^2$ | $4\ GeV^2$ |
| SI | $a_S x^{b_S}(1-x)^{c_S}(1+d_S\sqrt{x}+e_S x)$ | $a_S x^{b_S}(1-x)^{c_S}(1+e_S x)$ |
| NS | $a_N x^{b_N}(1-x)^{c_N}$ | $a_N x^{b_N}(1-x)^{c_N}(1+e_N x)$ |
| xg | $a_G x^{b_G}(1-x)^{c_G}$ | $a_G x^{b_G}(1-x)^{c_G}$ |
| input | $q_{val}$ from MRSD-' | gluon momentum fraction |
| charm | massless | $\gamma$ g fusion |

Table 1: Summary of QCD fit assumptions by ZEUS and H1

the quark and antiquark distributions. The assumptions for the QCD fits differ somewhat and are summarized in table 1. Attention has been paid to the correct treatment of errors although much remains to be done to understand the correlations of all parameters involved in those analyses.

As can be seen in figs. 1 and 2 the structure function behaviour *vs* $x$ and $Q^2$ is well reproduced by the QCD fit results. $F_2(x, Q^2)$ depends logarithmically on $Q^2$ in the covered large $Q^2$ range. There is no significant deviation observed from a continuous rise at low $x$. This is being investigated with new and more precise data around $Q^2 \simeq 5\ GeV^2$ and for $x$ near to $10^{-4}$. The data at large $Q^2$ are consistent with QCD based extrapolations from the fixed target data at higher $x$. In the large $Q^2$ region the increase of luminosity will be vital to study that question more precisely and also to measure further structure functions connected with $Z$ boson exchange [15].

The QCD analysis of scaling violations determines the gluon distribution $xg(x, Q^2)$ extending previous measurements to the region of very low $x \simeq 10^{-4}$. Fig. 3a comprises several determinations of $xg$ in leading order $\alpha_s(Q^2)$ of perturbation theory. The solid and dashed curves represent the QCD fit results from ZEUS and H1, respectively, which are in remarkable agreement. The data points are based on a consistency check where the DGLAP equation has been simplified by neglecting at low $x \leq 0.01$ the quark contribution to the scaling violations of $F_2$ and solving approximately the integral over $xg$ times the splitting function [16]. In this way one avoids the multiparameter fit and relates $\partial F_2/\partial lnQ^2$ directly to $\alpha_s \cdot xg$. Adopting the $\alpha_s$ value chosen by H1 to the ZEUS data one finds very good agreement between both experiments which means that both structure functions exhibit the same $Q^2$ dependence. Confirmation of this result comes from an H1 analysis of jet rates [17] which determines $xg$ from $\gamma g$ fusion processes (triangles in fig. 3a). H1 has performed a leading order QCD analysis introducing at low $x$ the BFKL gluon evolution equation ensuring smooth transition between the $xg$ distributions. This leads, based on the same data, to a gluon distribution even steeper than the DGLAP gluon, fig. 3a, although the description of the $F_2$ behaviour itself is very close to the pure DGLAP fit [13]. The NLO fit results, based on DGLAP only, are shown in fig.3b. Again both experiments analyses are in remarkable agreement. Note that the assumed shapes of $xg$ are very simple reflecting the still limited measurement accuracy rather than fundamental assumptions on the behaviour of $xg$. The fits somewhat prefer the low $x$ behaviour of $SI$ and $xg$ to be decoupled. Comparing with the expectation based on the extrapolated NMC result (solid curves at high $x$, fig. 3b) one indeed observes a large increase of $xg$ at low $x$.

Future, more precise structure function data and analyses of the final state will reveal whether the onset of new effects in the region of small distances but high parton densities can be seen at HERA. High luminosity and deuteron data will allow individual parton densities to be measured in the now opened kinematic range.

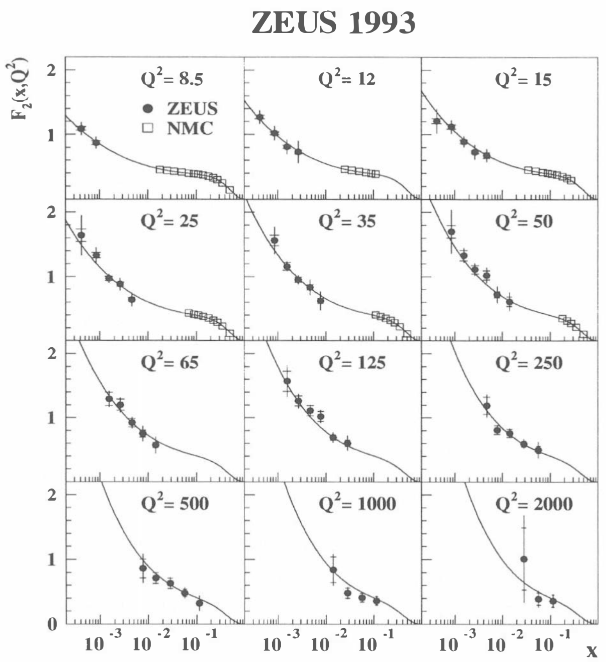


Figure 2: $F_2(x, Q^2)$ *measurement and NLO DGLAP QCD fit of ZEUS.*

**Acknowledgement** I would like to thank Tony Doyle, Aharon Levy and Stefan Schlenstedt for explanations on ZEUS results, Greg Bernardi, Albert DeRoeck, Thomas Naumann, Uta Stößlein and many friends in H1 for long, joint efforts to get $F_2$ and $xg$ and the Zeuthen H1 group, Joel Feltesse, Robert Klanner and Paul Söding for supporting my participation in a most interesting and pleasant rencontre with mountains rising even more spectacular than $F_2$.

## References

[1] H1 Collaboration, I. Abt et al., DESY 93-103 (1993).

[2] ZEUS Collaboration, M. Derrick et al., Phys.Lett. B293(1992)465; internal DESY report on ZEUS detector status, 1993.

[3] H1 Collaboration, T. Ahmed et al., Nucl.Phys. B439(1995)471.

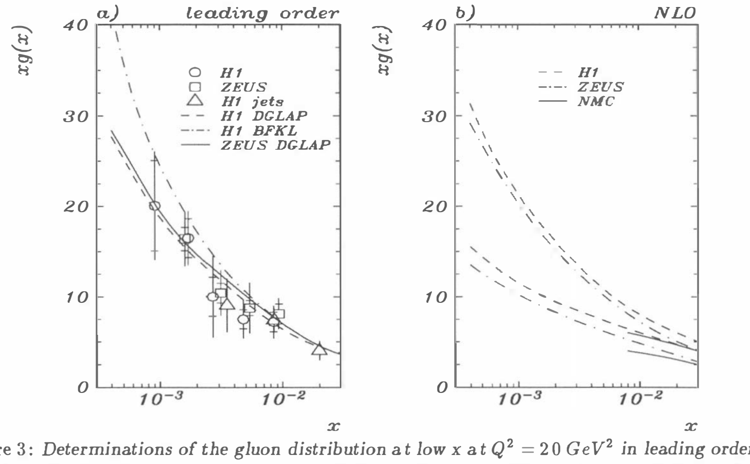


Figure 3: *Determinations of the gluon distribution at low x at $Q^2 = 20\ GeV^2$ in leading order (a) and NLO (b). The curves in fig. 3b denote the lower and upper limits for $xg$ as determined by the statistical and systematic error analyses.*


[4] ZEUS Collaboration, M. Derrick et al., Z.f.Phys. C65(1995)379.

[5] S. Bentvelsen, J.Engelen and P. Kooijman, Proc. Workshop 'Physics at HERA' vol.1, DESY 1992, p.23.

[6] NMC Collaboration, P .Amaudruz et al., Phys.Lett. B295(1992)159; CERN-PPE/92-124.

[7] BCDMS Collaboration, A.C. Benvenuti et al., Phys.Lett. B223(1989)485; CERN-EP/89-06.

[8] E665 Collaboration, A.V. Kotwal, Fermilab-Conf-95/046(1995) and these proceedings.

[9] A. De Rujula et al., Phys.Rev. D10(1974)1649.

[10] Yu.L. Dokshitzer, Sov.Phys. JETP 46(1977)641;
V.N. Gribov and L.N. Lipatov, Sov.J.Nucl.Phys. 15(1972)438 and 675;
G. Altarelli and G. Parisi, Nucl.Phys. 126(1977)297.

[11] E.A. Kuraev, L.N. Lipatov and V.S. Fadin, Sov.Phys. JETP 45(1977)199;
Y.Y. Balitsky and L.N. Lipatov, Sov.J.Nucl.Phys. 28(1978)282.

[12] L.V. Gribov, E.M. Levin and M.G. Ryskin, Phys.Rep.100(1983)1;
for recent developments of low $x$ theory see: Proc. Int. Workshop on DIS and Related Subjects, Eilat, Israel 1994, World Scientific Singapore, ed. by A.Levy.

[13] H1 Collaboration, T. Ahmed et al., DESY 95-81(1995), Phys.Lett. B to appear.

[14] ZEUS Collaboration, M.Derrick et al., Phys.Lett. B345(1995)576.

[15] M. Klein and T. Riemann, Z.f.Phys. C24(1984)151

[16] K. Prytz, Phys.Lett. B311(1993)286.

[17] H1 Collaboration, S. Aid et al., DESY 95-086 (1995), subm. to Phys.Lett.B.